Performance Characterization of the HYDROS™ Water Electrolysis Thruster

Karsten James, Todd Moser, Andrew Conley, Jeffery Slostad, Robert Hoyt
Tethers Unlimited, Inc.
11711 North Creek Parkway South, Suite D-113; (425) 486-0100
kjames@tethers.com

ABSTRACT

The HYDROS thruster uses a novel hybrid electrical/chemical propulsion scheme to enable CubeSats and other secondary payloads to perform missions requiring orbit agility and large ΔVs while launching with an inert, unpressurized, non-toxic propellant: water. The HYDROS thruster splits the water propellant on-orbit using electrical power to produce hydrogen and oxygen gas. The evolved gases are then combusted in a bipropellant thruster to provide high-thrust propulsion or utilized as cold gas to provide minimum impulse-bit thrust events. The addition of a larger gas volume to the current engineering test unit has allowed for more robust operation of the electrolyzer and longer thrust events. The parallel development of a torsional spring thrust stand allows for increased thrust and impulse measurement accuracy. Utilizing these tools we have conducted a detailed characterization of the electrolyzer and thruster performance. The electrolyzer characterization effort has demonstrated that the electrolyzer provides consistent and efficient performance across the range of upstream and downstream pressures and has demonstrated that electrolyzer wetting is the key predictor of electrolyzer performance. The thruster characterization effort has demonstrated high thrust (300-600 mN) performance and provided insight into potential design improvements moving forward.

INTRODUCTION

The increasing availability of secondary payload flight opportunities has led to a dramatic expansion in the use of small satellites for both commercial and science missions. Small satellite secondary payload missions of increasing complexity and with correspondingly increasing performance requirements are being proposed and flown. The HYDROS thruster, shown in Fig. 1, is a traditional bipropellant thruster designed for small satellite applications that generates hydrogen and oxygen fuel on orbit through the electrolysis of water.

Figure 1. HYDROS 1U Engineering Unit.

The use of an unpressurized, non-explosive, and non-toxic propellant makes HYDROS an ideal propulsion solution for secondary payload missions which are subject to launch constraints imposed by their host payloads. Additionally its 1U form factor allows it to integrate easily with a wide range of small satellite architectures.

Initially developed under a NASA Phase II SBIR contract Tethers Unlimited, Inc. (TUI) has matured the HYDROS thruster to TRL-5. Additional development has integrated an expanded gas volume to improve thruster performance. Current test and development efforts are focused on maturation of the HYDROS thruster to TRL-6 and beyond.

HYDROS Architecture

The HYDROS thruster is composed of four principle components: the water tank, a Proton Exchange Membrane (PEM) electrolyzer, gas storage volumes, and a bipropellant thruster. Water stored in the integrated water tank is deposited on demand onto the PEM electrolyzer. With the application of power the water is electrolyzed by a microgravity compatible process at power efficiencies up to 88%[1]. Hydrogen and oxygen gases are evolved and stored in separate gas volumes until they are mixed and combusted in the bipropellant microthruster. Integrated avionics provide

sensing and hardware control based on inputs from a microcontroller.

The design and sizing of each of the principal components of the HYDROS architecture has direct impacts on the performance of the HYDROS propulsion system. The modularity and scalability of the HYDROS design leads to a large design space over which system performance can be optimized to satisfy a wide range of possible mission requirements. However in order to fully understand and utilize this design space, the performance and capabilities of the electrolyzer and thruster must be well understood.

HYDROS Performance Characterization Effort

To better understand the HYDROS system and provide a basis for future design work TUI has conducted a test effort to characterize the performance of the HYDROS thruster and electrolyzer. A campaign of tests designed to isolate specific driving variables of the electrolyzer and thruster performance was undertaken following a concerted effort to design and build a thrust stand capable of measuring microNewton sized thrust events with characteristic times of up to several seconds. Investigations focused on electrolyzer characterization sought to determine the gas generation rate, efficiency, power requirements, and performance degradation of the electrolyzer under various operating conditions. Testing to characterize the HYDROS thruster remains incomplete pending complete calibration of the improved torsional spring thrust stand but early results are in line with previous thruster testing results.

ELECTROLYZER CHARACTERIZATION

In order to characterize the performance of the HYDROS electrolyzer several key test variables were identified and controlled during the test effort. Power input to the electrolyzer was controlled by supplying a constant current to the electrolyzer until the highest operating voltage of the electrolyzer was reached, at which point the voltage was maintained. The electrolyzer area, a key driver of gas evolution rate, was held constant throughout the test campaign but the larger electrolyzer of the current engineering unit allows comparative analysis of the impact of electrolyzer area with respect to past designs. The amount of water on the electrolyzer was a key variable of the test effort and was carefully controlled during testing. Finally, the operating pressure of the electrolyzer was measured to determine if it had any impact on electrolyzer performance.

The test plan developed for characterizing the electrolyzer controlled the starting tank pressures, the power input, and electrolyzer area to determine the effect of tank pressure and the amount of water on the electrolyzer on gas generation rates and power consumption. The test plan consisted of several

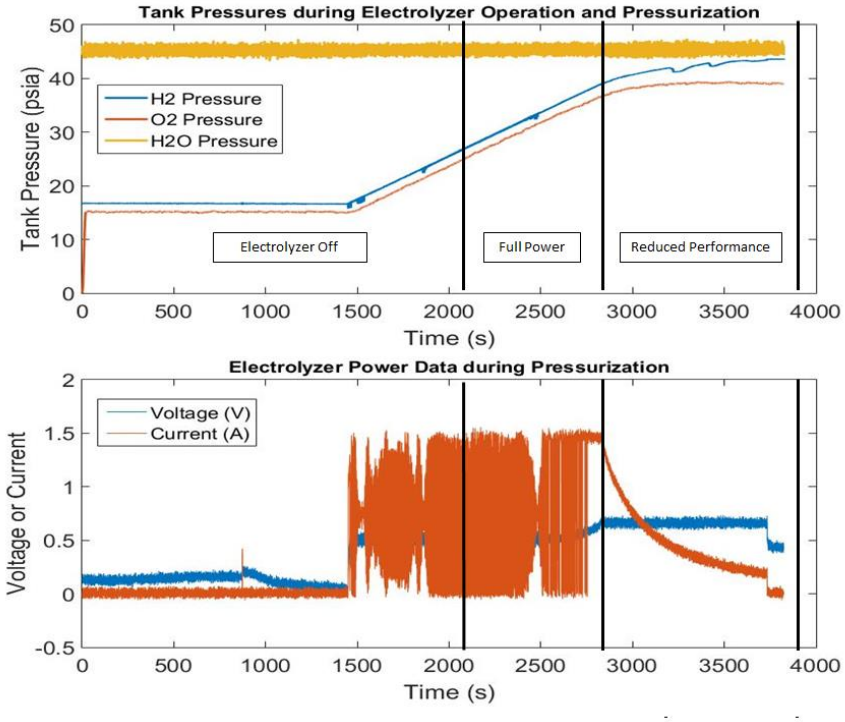

Figure 2. Baseline Electrolyzer Performance

iterations of wetting the electrolyzer with a known amount of water, waiting a predetermined time, and operating the electrolyzer until a predetermined cutoff pressure or until the electrolyzer current draw dropped below 0.5 amps and the electrolyzer was no longer effectively generating gas.

Electrolyzer Baseline Testing

Initial tests of the electrolyzer sought to determine the baseline performance of the electrolyzer. Figure 2 shows a typical pressurization of the gas volumes by the electrolysis of water. As expected when the electrolyzer is powered off the electrolyzer voltage and current are approximately zero. When HYDROS is commanded to pressurize the tanks, current is introduced to the electrolyzer and the power draw increases. Note that the current appears to fluctuate between 0A and 1.5 A. When monitored with a probe at the electrolyzer control circuit, the current is maintained at a constant 1.5 A when operating at full power; the fluctuations seen in Fig. 3 are caused by the difference in sample rates and resolution between the data acquisition hardware and the avionics. Operating normally the gas generation rate of the electrolyzer remains constant as it pressurizes the gas volumes while consuming approximately 2.25 W. After several minutes of operation the voltage increases slightly and the current decays. This change in power draw also corresponds to a decrease in gas evolution rate. Eventually the current drops to a level where gas generation ceases. Insufficient wetting of the electrolyzer was suspected as the root cause of this performance degradation which manifested itself with the addition of larger gas volumes.

It is important to note that there is a noticeable and unexpected difference between the oxygen and hydrogen tank pressures, particularly as the pressure in the gas volumes increases. The pressure measurements utilize different circuitry and calibration curves, resulting in different reported values. For the purpose of this analysis, only the hydrogen pressure measurement is considered based on development conducted on the instrumentation circuitry to improve performance and accuracy of the hydrogen pressure transducer.

Electrolyzer Wetting Analysis

Baseline electrolyzer testing suggested that wetting of the electrolyzer during operation would be necessary to achieve higher operating pressures with the expanded gas volumes. The second test effort sought to determine if insufficient wetting of the electrolyzer was the root cause of the performance degradation observed in the baseline testing. A test procedure was developed in which the electrolyzer would be initially wetted following the same procedure used in the baseline testing. Once degradation of the electrolyzer performance was observed the electrolyzer would be re-wetted and testing would continue. Figure 3 shows a

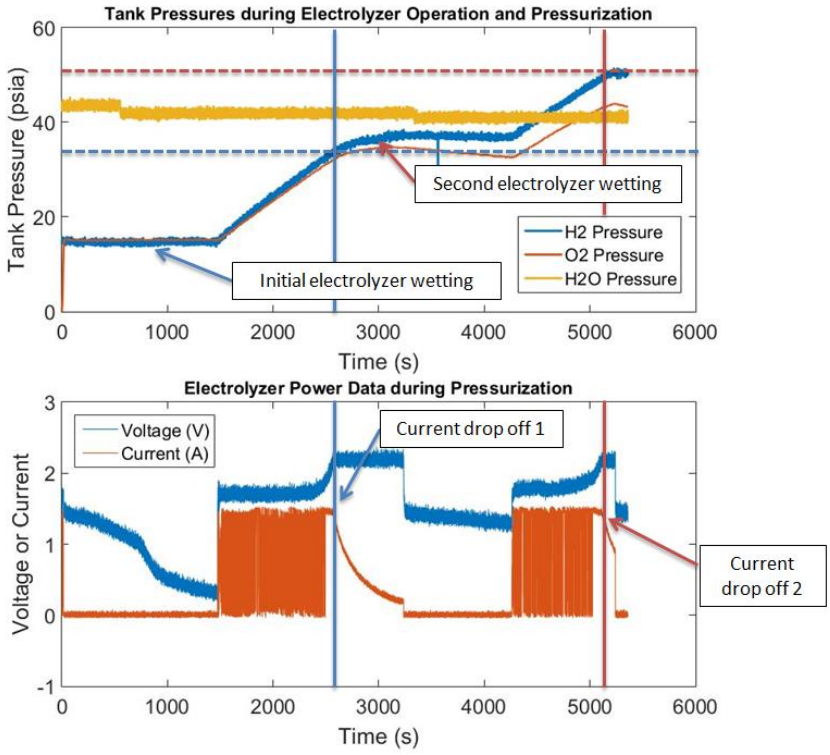

Figure 3. Electrolyzer Performance with Additional Wetting

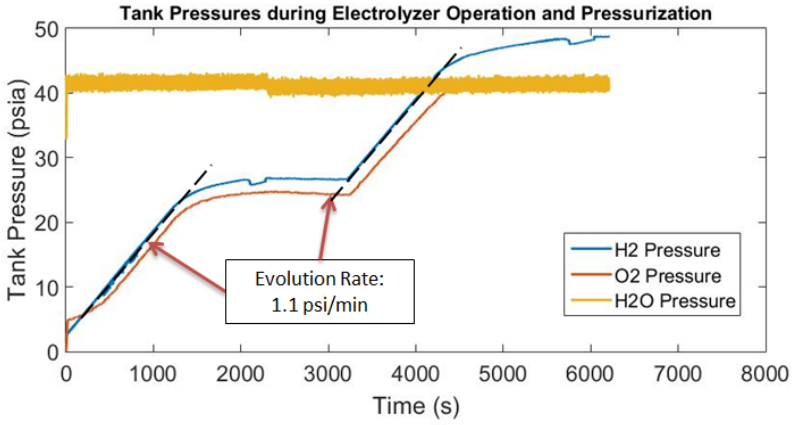

Figure 4. Electrolyzer Gas Generation Rates

typical result in which the electrolyzer was re-wetted once during the gas pressurization procedure. As demonstrated in Fig. 3 secondary wettings allowed the electrolyzer to evolve more gas, each one increasing the gas tank pressures an additional 20 to 25 psi. These results confirmed that the amount of water on the electrolyzer drives the electrolyzer's performance under a constant current and insufficient wetting of the electrolyzer is the root cause of the performance degradation observed in our baseline testing.

Examining the performance degradation of the electrolyzer as water is consumed both before and after additional wetting it is clear that the performance of the electrolyzer decays in a predictable manner. Once the electrolyzer reaches a condition in which there is insufficient wetting of the PEM the gas evolution rate decreases in parallel with a simultaneously current drop. The current drop, therefore, can be used to trigger a scheme for supplying additional water to the electrolyzer on demand to maintain a constant gas generation rate.

Gas Evolution Rate

While our first test plan demonstrated that performance of the electrolyzer depended largely on sufficient wetting of the PEM, the possibility of gas tank pressure affecting the gas evolution rate also needed to be investigated. By examining the rates of different tests with multiple wettings, such as the one shown in Fig. 4, it can be seen that the gas evolution rate is successfully restored with additional wettings, independent of the starting gas tank pressure below 50 psi, the highest pressure investigated in this test effort.

Following an extensive test campaign across a range of conditions and modes of operation the electrolyzer design for the current HYDROS engineering unit was well characterized. This characterization coupled with previous investigations provides an ideal basis for further analytical model development and serves as an important reference for future design efforts.

THRUST STAND

Early HYDROS development and test efforts highlighted the need for more precise measurement of thrust events in order to obtain repeatable and accurate thruster performance data. There are few widely used thrust stand configurations that meet the programmatic needs of the HYDRO test effort, including a hanging pendulum, inverted pendulum, torsional spring pendulum, or null-force balance. Each method has particular benefits and constraints and the selection of an appropriate test stand architecture depends heavily on the requirements of the test effort.

Thrust Stand Selection

The HYDROS thruster is categorized as a microNewton bipropellant thruster suitable for use in small spacecraft platforms. Due to the limited gas volumes thrust events occur at characteristic time scales of 0.1 seconds to 2.0 seconds. A thrust stand developed to characterize the HYDROS thruster must therefore respond to microNewton stimuli of short duration. The short duration of the thrust events mean the thrust characteristics and fluid flow remain in a dynamic state and steady state operations are not expected. For this reason, a null-force balance, which relies on balancing the unknown force of the thruster with a known force, is not applicable. A thruster mounted to a hanging or inverted pendulum moves in a direction that is affected by gravity. While the mass of the thruster could be easily characterized before each test, the rapidly changing thruster configurations involved in the research and development process called for a more stable and repeatable measurement system.

A torsional spring thrust stand was selected for its sensitivity and the independence of its setup and results from the mass of the thruster. When an external (thrust)

force acts on a torsional pendulum stand, the stand deflects perpendicularly to the gravity vector, negating the effect of thruster mass on the deflection. Once deflected by either a sustained or impulsive force the thrust stand oscillates due to the restorative force provided by a pair of torsional springs.

Torsional Thrust Stand

The torsional thrust stand constructed for the HYDROS characterization effort, diagramed in Fig. 5, consists of two arms branching from each side of a center axis. The thruster mounts to the left arm, a counter weight is mounted on the end of each arm. The center axis is mounted to a frame via two torsional springs. The frame rests on an optical table inside a vacuum chamber, and is isolated from the environmental vibrations by three rubber feet. The optical table is adjusted to keep the thruster level during operations to ensure that the thrust vector and displacement of the arms remain perpendicular to the gravity vector. When the thruster is fired, the thrust displaces the arms. The displacement is measured by the linear displacement sensor (LDS) and recorded by a LabVIEW VI.

In order for the thrust measurement to be accurate the thrust event must appear impulsive to the thrust stand. To achieve this the natural period of the thruster must be at least an order of magnitude greater than the length of the thrust event being measured[2]. This condition was satisfied through selection of the arm length, counterweight masses, and stiffness of the torsional springs. The natural period of the thrust stand's damped oscillation was then measured using the LDS.

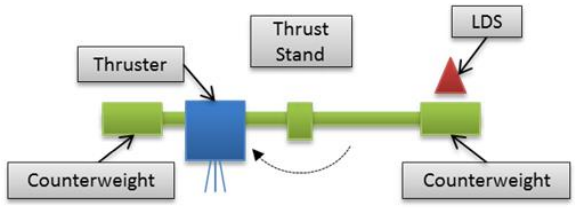

Figure 5. Top-Down View of the Thrust Stand

Thrust Stand Calibration

After selecting and constructing the appropriate thrust stand, a proper calibration was performed to determine the thrust stand's response to a known force. With this calibration, the effects of the thruster can be correlated to the known force, permitting the calculation of the thruster performance characteristics.

The calibration of the torsional thrust stand requires a small hammer capable of applying and measuring a force. This hammer is used to tap the arm of the thrust stand and measure the applied impulse with an integrated piezoelectric force transducer. The fixed distance from the center axis to the hammer and the fixed distance from the center axis to the thruster allow the forces can be correlated according to,

$$(F \cdot l)_{hammer} = (F \cdot l)_{thruster}, \tag{1}$$

where F and l are the force applied and distance to the center axis by either the hammer or thruster.

To automate several aspects of the calibration process, including applying the force with the hammer and calculating the constants of correlation, three programs were used. First, an Arduino and its associated programming software were used to apply a consistent impulse to the thrust stand. Second, a LabVIEW VI was used to record and output the LDS and force transducer data taken during the calibration. Finally, a MATLAB script was written to quickly process the calibration data and output the calibration curve.

Thrust Stand Error Analysis

As with any laboratory measurement, there is uncertainty in the thrust measurements provided by the torsional thrust stand. To better understand the uncertainty of the thruster's reordered performance a detailed error analysis was conducted.

Calibration and measurement error are the two primary sources of uncertainty in the torsional spring system. Errors arising from these uncertainties must be qualified and propagated through the system in order to determine the error in the resultant impulse and thrust measurements. Due to the linear nature of the piezoelectric force transducer's output the calibration uncertainty is contained in the constants (m and b) of the general linear form,

$$y = mx + b. \tag{2}$$

Here, the differences between the individual data points and the linear equation and the number of data points N, can be used to calculate σ_m and σ_b, the absolute uncertainties in the slope and offset constants.

$$\sigma_y = \sqrt{\frac{1}{N-2}\sum(y_i - b - mx_i)^2}$$

$$\sigma_b = \sigma_y \cdot \sqrt{\frac{\sum x^2}{N\sum x^2 - (\sum x)^2}}. \tag{3}$$

$$\sigma_m = \sigma_y \cdot \sqrt{\frac{N}{N\sum x^2 - (\sum x)^2}}$$

The absolute uncertainty in the calibration, coupled with the uncertainty in the thrust stand displacement $\delta\theta$, and calibration slope σ_m can be used to determine the relative uncertainty in the impulse bit,

$$\delta I_{bit} = \frac{\sqrt{\left(m\Delta\theta\sqrt{\left(\frac{\sigma_m}{m}\right)^2 + \left(\sqrt{2}\delta\theta\right)^2}\right)^2 + \sigma_b^2}}{I_{bit}}. \quad (4)$$

The uncertainty in the average thrust can be directly related to the uncertainty in the impulse bit,

$$\delta\, Thrust_{avg} = \delta I_{bit}. \quad (5)$$

Finally the uncertainty of the specific impulse can be calculated according to the following algorithm:

$$\delta n_{H_2} = \sqrt{\delta P_{H_2}^2 + \delta V_{H_2}^2}$$

$$(\delta m_{H_2} = \delta n_{H_2}) \;=\; (\delta n_{O_2} = \delta m_{O_2})$$

$$\delta m_{gas} = \sqrt{\delta m_f^2 + \delta m_i^2}, \quad (6)$$

$$\delta \dot{m}_{gas} = \sqrt{2} \cdot \delta m_{gas}$$

$$\delta I_{sp} = \sqrt{\delta\, Thrust_{avg}^2 + \delta \dot{m}_{gas}^2}$$

where the uncertainty is a function of the errors in the pressure δP_{H_2}, volume δV_{H_2}, and thrust $\delta Thrust_{avg}$ values.

The relative error of each thruster performance metric (specific impulse, average thrust, and impulse bit) is driven mainly by the noise in the linear displacement sensor measuring the deflection and in the hydrogen pressure transducer. The noise in both signals occurs at constant amplitudes, resulting in significantly higher uncertainties when either the pressure or the deflection of the thrust stand arms is small. In order to measure with good accuracy thrust events should be sized to ensure the gas storage volumes experience a pressure drop of several psi and the deflection results in a 1 Volt peak-to-peak voltage oscillation from the linear displacement sensor.

THRUSTER CHARACTERIZATION

Preliminary thruster testing at ambient pressure and in vacuum has increased our confidence in the design's reliability and performance. We utilized the gases evolved during the electrolyzer testing campaign to begin characterizing thruster valve and ignition timings, characteristic pressures, and approximate thrust values. This testing occurred in parallel with the development and refinement of the thrust stand and needed design changes to the thrust stand invalidated much of the thruster performance test data. Initial thrust results are presented here while further testing and design modifications remain ongoing. The addition of expanded gas volumes prevented the installation of a pressure transducer in the combustion chamber of the thruster. Previous test efforts have used chamber pressure data to help characterize the thrust performance. In lieu of this information thrust data has been measured as a function of the pressure drop in the gas volumes for each thrust event.

In order to determine specific impulse the mass flow rate, it was critical that we understood how valve timing and initial tank pressure—two user-defined values—contributed to the amount of mass ejected during the thrust event. As with the thrust characterization of the mass flow rate is continuing but has been setback by multiple instrumentation issues.

Determining Thrust

Using the calibrated thrust stand developed and configured for the proper thrust event length, the impulse bit of each thrust event can be determined according to,

$$I_{bit} = m \cdot D + b, \quad (7)$$

where I_{bit} is the impulse bit in Newton-seconds, m and b are the calibration parameters previously discussed, and D is the peak-to-peak displacement of the thrust stand in Volts. Next, using the duration for which the gas valves are open *t* as the length of the impulse event, the average thrust can be determined according to,

$$T_{avg} = \frac{I_{bit}}{t}. \quad (8)$$

After several recorded thrust events, the initial average thrust values were compiled and can be seen in Fig. 6. These results are preliminary and calibration and

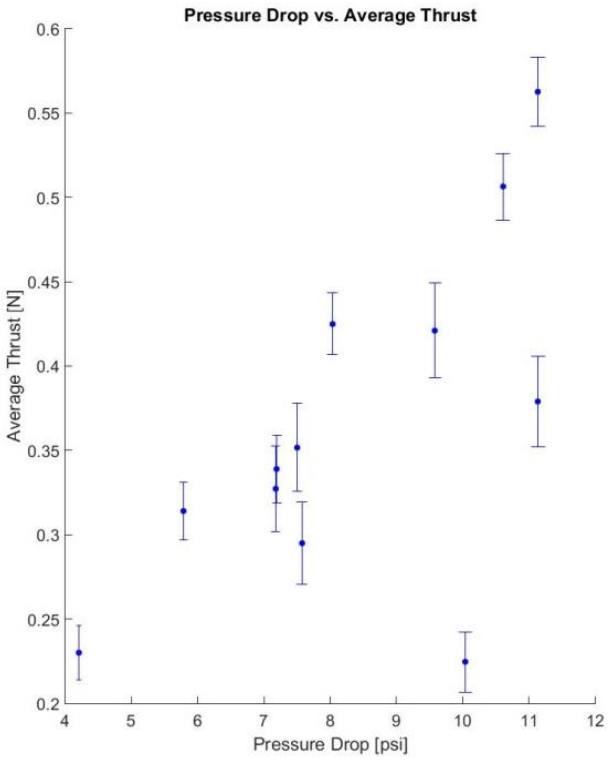

Figure 6. Initial Thrust Data

qualification of the thrust stand and test hardware remains ongoing.

Using the average thrust, the specific impulse can be calculated according to,

$$I_{sp} = \frac{T_{avg}}{g_o \cdot \dot{m}}, \quad (9)$$

where g_o is the gravitational constant at the Earth's surface, and $\dot{m}$ is the mass flow rate through the nozzle. Similar thrust levels recording during previous test efforts resulted in an average I_{sp} of 258 seconds[3] however questions about the mass flow rate of the current unit have prevented a characterization of the current I_{sp}.

The thrust values exhibited the expected trend: as the pressure drop increases, the average thrust also increases. A greater pressure drop indicates that more gas is released, as the change in tank pressure is directly proportional to the mass expelled by the thruster. A greater amount of fuel corresponds to higher expected thrust levels. The data shown in Fig. 6 demonstrates that thrust levels approaching 600 mN are achievable. While we are confident in the process of calculating the thrust, we experienced several instrumentation issues including noise in the LDS and pressure circuits, as well as in the difficulty in accurately determining the thrust event length.

CONCLUSION

While the average thrust values are promising this test campaign has demonstrated that improvement of the HYDROS thruster design is possible. TUI is seeking to continue development efforts to realize these potential design enhancements through continued test and evaluation including supporting investigations of thruster and nozzle design improvements. A design optimization study is expected to begin in the coming months to help characterize system performance and develop design tools that will aid in future development efforts. Additional avionics and test hardware improvements are sought to add additional pressure sensors, as well as more powerful data acquisition units to make testing more effective and produce more accurate and precise results.

Despite testing hurdles HYDROS continues to demonstrate its potential to provide orbital agility to small satellites using water propellant. The HYDROS architecture is uniquely suited to provide compelling propulsion solutions for a wide range of needs including orbital maneuvering, attitude control, orbit maintenance, and end of life deorbit.

Acknowledgments

The authors would like to acknowledge the NASA SBIR program for providing funding for the HYDROS thruster under contract NNX12CA09C. The authors would also like to acknowledge the Air Force Institute of Technology for their ongoing support and test efforts.

References

1. J.S. Wrobel, et al., "PowerCube™ - Enhanced Power, Propulsion, and Pointing to Enable Agile, High-Performance CubeSat Missions." AIAA Space 2012 Proceedings, Pasadena, CA (Sept. 2012).
2. Polk, James E., et al., "Recommended Practices in Thrust Measurements." No. IEPC-2013-440. California Institute of Technology Pasadena Jet Propulsion Lab, 2013.
3. K. Liu, et al., "HYDROS™ Thruster Component Testing in Atmospheric and Simulated Space Environment" Forthcoming paper, AIAA Dayton Cincinnati Aerospace Sciences Symposium.